AJNR

Automated CT Segmentation and Analysis for Acute Middle Cerebral Artery Stroke

Joseph A. Maldjian, Julio Chalela, Scott E. Kasner, David Liebeskind and John A. Detre

AJNR Am J Neuroradiol 2001, 22 (6) 1050-1055
http://www.ajnr.org/content/22/6/1050

AJNR Am J Neuroradiol 22:1050–1055, June/July 2001

Automated CT Segmentation and Analysis for Acute Middle Cerebral Artery Stroke

Joseph A. Maldjian, Julio Chalela, Scott E. Kasner, David Liebeskind, and John A. Detre

BACKGROUND AND PURPOSE: **The quantitative nature of CT should make it amenable to semiautomated analysis using modern neuroimaging methods. The purpose of this study was to begin to develop automated methods of analysis of CT scans to identify putative hypodensity within the lentiform nucleus and insula in patients with acute middle cerebral artery stroke.**

METHODS: **Thirty-five CT scans were retrospectively selected from our CT archive (scans of 20 normal control participants and 15 patients presenting with acute middle cerebral artery stroke symptoms). The DICOM data for each participant were interpolated to a single volume, scalp stripped, normalized to a standard atlas, and segmented into anatomic regions. Voxel densities in the lentiform nucleus and insula were compared with the contralateral side at $P < .01$ using the Wilcoxon two-sample rank sum statistic, corrected for spatial autocorrelation.**

RESULTS: **The quality of the registration for the anatomic regions was excellent. The control group had two false-positive results. The patient group had two false-negative results in the lentiform nucleus, two false-negative results in the insular cortex, and one false-positive finding for the insular cortex. The remainder of the infarcts were correctly identified. The original clinical reading, performed at the time of presentation, produced five false-negative interpretations for the patient group, all of which were correctly identified by the automated algorithm.**

CONCLUSION: **We present an automated method for identifying potential areas of acute ischemia on CT scans. This approach can be extended to other brain regions and vascular territories and may aid in the interpretation of CT scans in cases of hyperacute stroke.**

CT is the primary imaging technique for cases of hyperacute stroke, and it is the requisite diagnostic modality before the initiation of therapy with IV administered recombinant tissue plasminogen activator. The CT changes of acute infarction can be subtle within the first several hours of symptom onset. These findings include hypodensity with loss of gray-white differentiation and effacement of sulci. The CT indicators of acute ischemia are related to edema, which causes a decrease in the attenuation of involved structures (1, 2). Density changes have been found to be the most frequent sign of early ischemia (3–5). One of the most sensitive indicators of acute middle cerebral artery (MCA) ischemia is loss of the insular ribbon (5). The hyperdense MCA sign has also been reported as a sign of acute ischemia, in which high attenuation blood clot is identified within the MCA as it traverses the sylvian fissure. This sign, however, has limited value, especially with modern CT scanners, with which the MCA frequently appears bright, even in normal patients (6). Other indicators of acute stroke include loss of gray-white differentiation, especially in the region of the basal ganglia and internal capsule (7). Sulcal effacement can result from cortical swelling, which decreases the size of the CSF spaces surrounding affected gyri (8). Although these signs can be confidently identified by a neuroradiologist (9), they are relatively subtle and can easily be missed or misinterpreted by other physicians, even those specifically trained in the treatment of patients with acute stroke.

The importance of accurate interpretation of CT scans in cases of hyperacute stroke is related to the appropriate triage of patients for stroke interventions. Recombinant tissue plasminogen activator has been approved by the United States Food and Drug Administration for therapy of stroke within 3 hours of symptom onset. Presently, the decision to treat patients with recombinant tissue plasminogen activator relies on the duration of symptoms and results of CT. Secondary analysis of data from the

Received August 22, 2000; accepted after revision December 10.

From the Departments of Radiology (J.A.M.) and Neurology (J.C., S.E.K., D.L., J.A.D.), Hospital of the University of Pennsylvania, Philadelphia, PA.

Research support was provided by the American Roentgen Ray Society Scholars Program 1999–2000 (J.A.M.).

Address reprint requests to Joseph A. Maldjian, MD, Division of Radiologic Sciences, Wake Forest University School of Medicine, Medical Center Boulevard, Winston-Salem, NC 27157.

National Institute of Neurological Disorders and Stroke recombinant tissue plasminogen activator trial and results from the European Cooperative Acute Stroke Study trial suggest that CT findings of changes involving >33% of the MCA territory are associated with increased incidence of intracranial hemorrhage and may pose a relative contraindication to its use (10, 11). Thus, many stroke clinicians have adopted the practice of excluding patients for recombinant tissue plasminogen activator with CT evidence of major (>33%) involvement of the MCA territory. Patients with >50% MCA territory hypodensity revealed by CT are at high risk for the development of fatal herniation (12). These patients may benefit from even more aggressive interventions, such as decompressive surgery, with hemicraniectomy and durotomy, or induced hypothermia.

Numerous studies have shown inadequate interpretation of CT scans by acute care physicians in cases of acute stroke (13–15). This is a serious problem because it may lead to inappropriate treatment of these patients with thrombolytic agents, which can result in major complications, including intracranial hemorrhage, brain herniation, and, ultimately, death. It has been shown that there is wide interrater variability in the interpretation of CT scans by acute care physicians, neurologists, and residents (14, 15). Although in the ideal setting, experienced neuroradiologists would be interpreting all CT scans in cases of acute stroke, the reality is that in many settings, neuroradiologists are not involved in the immediate decision-making process. A recent study by Grotta et al (15) showed a considerable lack of agreement among experienced clinicians in recognizing and quantifying early CT changes of acute stroke. Raters included National Institute of Neurological Disorders and Stroke trial investigators, other neurologists, other emergency medicine physicians, and radiology and stroke fellows. Neuroradiologists were specifically excluded from the group. Previous studies have shown excellent agreement among neuroradiologists for recognition of early CT changes (9, 16, 17). In another recent study, it was shown that intracranial hemorrhage can be missed on CT scans by the treating emergency physicians (14). Thus, there is considerable lack of agreement among experienced clinicians in recognizing and quantifying CT changes in cases of acute stroke.

The quantitative nature of CT should make it amenable to semiautomated analysis using modern neuroimaging methods, which could be used to assist physicians in the acute interpretation of these cases. During the past decade, major advances have been made in the development of computerized image analysis tools. These include methods for automated normalization, segmentation, and regional signal analysis. However, application of these image analysis methodologies for CT has largely been ignored. One group has applied simple subtraction of histograms of the entire hemispheres on CT scans and has shown a significant increase in detection rate for acute infarcts (18). This method, however, does not take into account regional differences in attenuation, asymmetries in scan plane, and patient orientation and cannot be used to quantify infarct volumes. In a recent study by Lev et al (17), it was found that merely adjusting the window and level settings can improve the sensitivity to acute stroke identification on CT scans.

The purpose of our study was to use automated image analysis to assess regional hypodensity on CT scans obtained of patients presenting with acute MCA infarction. We think that the use of modern image analysis tools can assist in the interpretation of hyperacute CT scans. As an initial implementation of this approach, we assessed hemispheric differences in hypodensity in the insula and lentiform nucleus and compared the results with the initial clinical interpretation of the scans.

Methods

Fifteen CT scans were retrospectively selected of patients presenting with acute stroke symptoms to the Division of Stroke and NeuroCritical Care at our institution. The patients were found to have had strokes on the basis of clinical symptoms and follow-up imaging (performed within 36 hours of acute presentation). Scans lacking significant motion and beam-hardening artifacts were chosen. Twenty CT scans of patients presenting for workup of headache were also selected as a control group. DICOM CT data were digitally transferred to off-line workstations for postprocessing. All scans (including those of the control group) were reviewed by a neuroradiologist to document any findings of acute MCA territory stroke. All postprocessing was performed using routines written in IDL (Research Systems Inc., Boulder, CO).

Image Preprocessing

At our institution, CT is routinely performed using a 512 × 512 matrix and a 24-cm field of view, with 3-mm axial cuts through the posterior fossa and 10-mm cuts through the supratentorial space. Although the cuts may be contiguous, they represent two distinct volumes with different pixel dimensions through a single brain. Before the CT volume can be normalized, it must be interpolated into a single CT volume of uniform section thickness. Using header information within the DICOM images, we developed an IDL routine that computes the affine transformation between the infratentorial volume and the supratentorial volume. A single CT volume is then generated and interpolated to 5-mm section thickness and 256 × 256 matrix size.

Scalp Stripping

For normalization routines to work optimally, extraneous features must be removed from the data sets. This includes all data outside the brain. The skull is a source of potential error, as are structures such as the headholder and gantry, which are included in the CT field of view. We developed an IDL routine that uses thresholding (bone has attenuation values 20–30 times higher than that of brain) and local clustering to remove the skull. The routine automatically identifies ''seed voxels'' within the brain (based on attenuation and spatial location near the center of the volume). The scalp stripping takes approximately 30 seconds on a 300-MHz Sun Microsystems Ultra 10 unit.

TABLE 1: Control group histogram *P* values

Subject	Lent*	Insula
1	0.203488	0.157389
2	0.0633152	0.367663
3	0.142475	−0.0023301
4	0.396714	0.0653985
5	0.00726187	0.5
6	0.323384	0.101664
7	0.197371	0.118371
8	0.37171	0.136932
9	0.102817	0.0525244
10	0.11085	−0.0171999
11	−0.0350543	0.485807
12	−0.0103583	0.177435
13	0.03180587	0.466162
14	0.137617	0.194093
15	−0.0201214	0.129282
16	0.363489	0.0171193
17	0.128244	0.422418
18	−0.0137622	0.0853457
19	−0.0223427	0.179902
20	0.222504	0.402358

Note.—Negative values indicate involvement of the left side.
* Lent: lentiform nucleus.

Image Normalization

The scalp-stripped interpolated CT volumes were normalized to a standard atlas in Talairach space (19) using an SPM99-based normalization module (20, 21). The routine uses a T1-weighted MR image as the template, although a CT template, once developed, can be used instead.

Image Segmentation

We have previously normalized an anatomic regional atlas (22) to our Talairach template. The regional atlas information was applied to the normalized CT scan to generate regional data on the basis of anatomic location. Regions included the right and left lentiform nucleus (globus pallidus plus putamen), internal capsule, and insula.

Statistical Analysis

Histograms of the voxel density distributions were generated, and the voxel densities in the lentiform nucleus and insula were compared with the contralateral side using the Wilcoxon two-sample rank sum statistic. A non-parametric statistic was used because the distribution of attenuation change may display a non-gaussian distribution, unless the whole region is involved. The neighboring voxels within a region are not truly independent of each other (ie, they may be functionally connected and may share vascular supply). The regions were therefore resampled using an 8×8 smoothing kernel before conducting statistical analysis to correct for spatial autocorrelation. A cutoff of $P < .01$ was arbitrarily set for determination of significant hypodensity.

Results

The automated scalp stripping, normalization, and segmentation were successful in all cases (as assessed by visual inspection). The quality of the registration for the anatomic regions was also excellent for both the patients and the healthy control participants, with the insular and lentiform regions automatically placed at their expected locations. Each automated analysis was accomplished within 10 minutes on a SUN Ultrasparc10 workstation.

The results of the automated segmentation analysis for the control participants are summarized in Table 1. In the control group, there was one false-positive finding for the lentiform nucleus (control participant 5) and one false-positive finding for the insula (control participant 3). Neither of these cases showed evidence of atrophy or previous infarction in these regions. Note that the false-positive results for the control participants barely achieved levels of statistical significance.

The results of the automated segmentation analysis for the patient group are summarized in Table 2. In the patient group, 12 of the 15 cases involved the lentiform nucleus (Table 2). The automated analysis correctly identified all of these infarcts, except for two false-negative findings.

TABLE 2: Patient histogram *P* values and CT interpretations

Subject	Lent*	Insula	Hours	Initial Reading	Follow-up Scan
1	0.203488	−1.00E-09	12–24	Left insula	Left insula, some lentiform
2	0.00130022	−4.61E-05	<6	? Left parietal	Right lentiform
3	2.32E-06	0.121933	6–12	Right MCA	Right insula and lentiform
4	2.32E-06	1.00E-09	12–24	Right MCA	Right insula and lentiform
5	0.0385668	4.17E-07	<6	Normal	Right insula and lentiform
6	0.166294	−0.0014378	<6	Left insula	Left insula
7	−1.00E-09	−1.57E-04	<6	? Left insula	Left Insula and lentiform
8	0.0097734	0.377767	<6	Normal	Right MCA
9	0.0302814	9.83E-03	<6	? Right insula	Right insula
10	−1.46E-04	−3.339E-04	<6	Normal	Left MCA
11	2.32E-0.6	1.00E-09	12–24	Right MCA	Right MCA
12	2.32E-0.6	1.73E-06	6–12	Right MCA	Right insula and lentiform
13	−2.32E-06	−1.00E-09	6–12	Left lentiform	Left lentiform and insula
14	−5.25E-06	−2.98E-07	12–24	Left MCA	Left lentiform and insula
15	0.163055	1.8E-04	<6	Normal	Right insula

Note.—Negative values indicate involvement of the left side.
* Lent, lentiform nucleus.

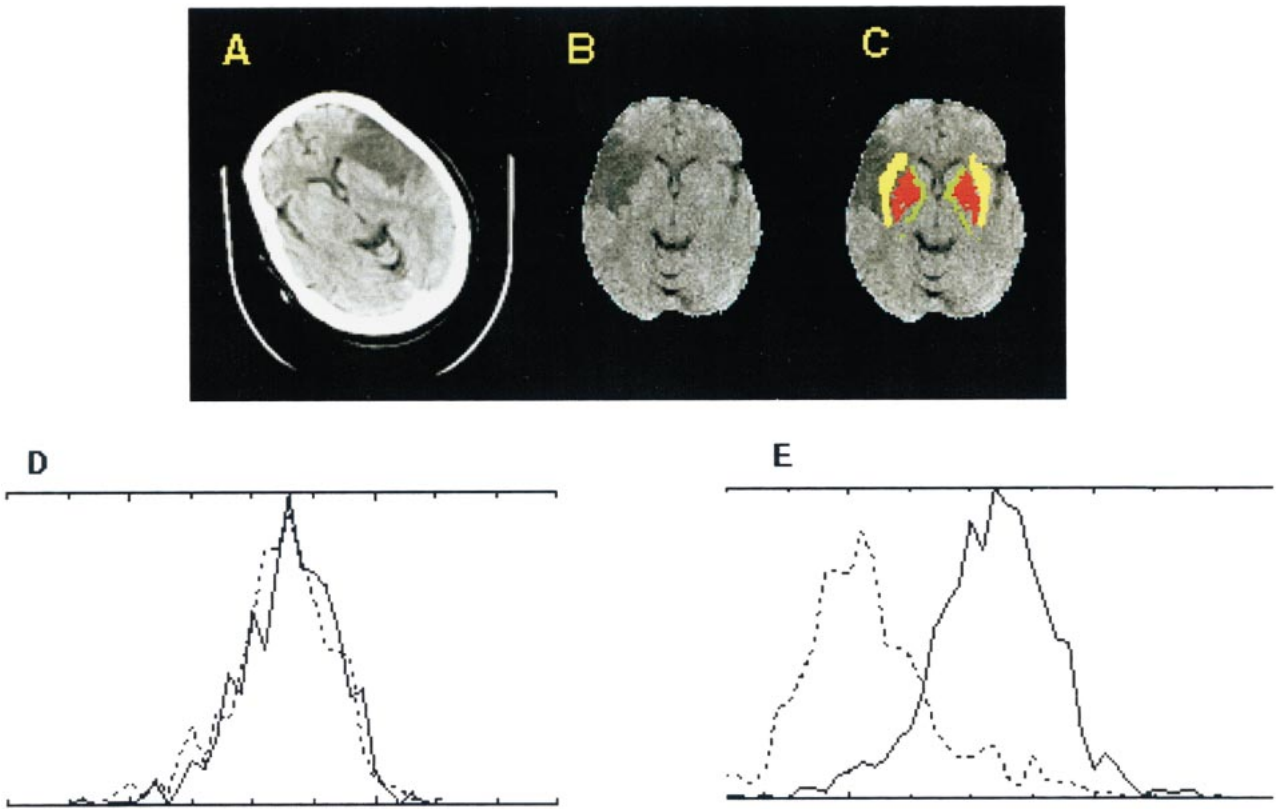

FIG 1. Large left MCA stroke (patient case 1).

A, Raw CT scan shows left MCA infarct predominantly involving the insula, with marginal involvement of the lentiform nucleus (*right* of image is left of patient).

B, CT scan after automated scalp stripping and normalization to Talairach atlas (*right* of image is right of patient).

C, Automated segmentation color coded onto normalized CT scan shows excellent registration of lentiform nucleus (*red*) and insular cortex (*yellow*). Internal capsule is displayed in *green.*

D, Histogram plot for lentiform nucleus shows mild leftward shift for the left lentiform nucleus (*dotted line, P* < .0196 using a Wilcoxon statistic corrected for spatial autocorrelation).

E, Histogram plot for insula shows a large leftward shift ($P < 1 \times 10^{-9}$).

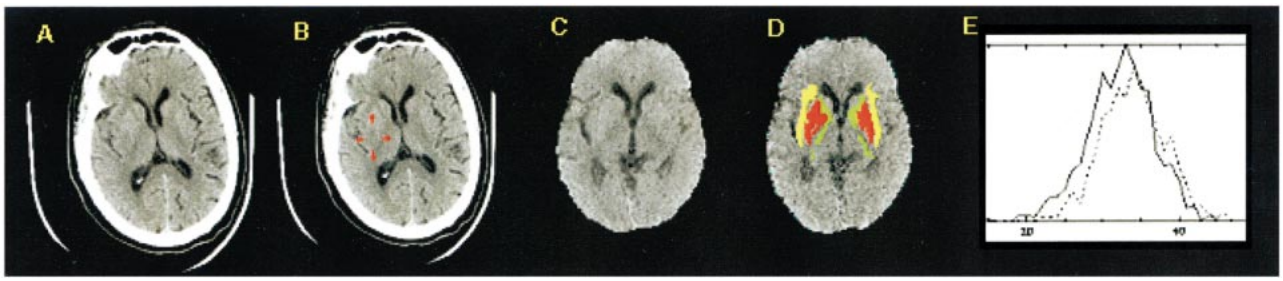

FIG 2. Subtle right MCA stroke (patient case 5).

A, Raw CT scan shows subtle right MCA territory infarct (*right* of image is left of patient) involving the insula and posterior putamen.

B, Posterior putamen and insula are highlighted.

C, CT scan after automated scalp stripping and normalization to Talairach atlas (*right* of image is right of patient).

D, Automated segmentation color coded onto normalized CT scan (as in Fig 1) shows excellent registration of basal ganglia structures and insular cortex.

E, Histogram plot for insula shows leftward shift for the right insula (*solid line,* $P < 1 \times 10^{-9}$).

One of the false-negative cases showed only marginal involvement of the basal ganglia (patient case 1), with predominant involvement of the insula (Fig 1). Fourteen of the patient cases involved the insula. The automated analysis identified all of these infarcts correctly, with one false-positive finding.

The performance of the automated analysis is summarized in Table 3. The original reading, performed at the time of presentation, produced five false-negative interpretations for these cases. All these cases showed subtle findings of infarction in the MCA territory, and all were correctly identified using the automated analysis methodology.

TABLE 3: Automated CT analysis summary for the patient group

	Lentiform nucleus		Insular Cortex	
	Infarct+	Infarct−	Infarct+	Infarct−
CT analysis +	10	0	12	1
CT analysis −	2	3	2	0

Figure 2 shows an example of a CT scan of a patient with a subtle right MCA infarct that was missed at the time of the initial reading. There was hypodensity involving the posterior portion of the insula and putamen on the right side, with loss of gray-white differentiation. The histogram plot for the anatomic segmentation shows a significant leftward shift for the insular cortex ($P < 4 \times 10^{-7}$).

Discussion

In this study, we show an automated method for identifying areas of acute ischemia on CT scans. This approach can successfully identify hypodensity within the insula and lentiform nucleus. The entire process takes approximately 10 minutes on a modern workstation. We chose to limit our analysis to the regions of the lentiform nucleus and insula because these are the areas most commonly involved by MCA infarcts. The approach presented herein can be extended to more anatomic regions and to characterization of vascular territories. This may provide a semiautomated method for quantification of infarct volumes and may be of value in triage for recombinant tissue plasminogen activator and in predicting stroke outcomes. In a recent article by Barber et al (23), it was shown that a quantitative stroke scale based on parcellation and scoring of CT scans in cases of early stroke predicts functional outcome and symptomatic intracerebral hemorrhage. The article provides further evidence that more accurate quantification of infarct volumes can be helpful in the determination of stroke therapies and outcomes. The method used, however, is manually intensive, requiring a human observer reporting on subregions within a vascular territory, with each subregion determined subjectively by the observer. These are all steps that can be performed in an automated fashion, potentially by an optimized version of our methodology. Currently, there is an intensive effort to better define the ischemic penumbra (ischemic regions that have not yet infarcted and are amenable to treatment). Much of this research involves MR imaging, which is inconvenient to perform in the acute setting. Improved CT analysis, in combination with other emerging CT methodologies (xenon-enhanced CT perfusion, CT angiography) may allow the penumbra to be identified by CT.

In this small population of CT scans in cases of hyperacute stroke, our algorithm performed at least as well as the initial radiologic interpretation, and in several cases, it was able to identify acute infarcts that were initially missed. Although there were several false-positive interpretations for the control group, the levels of statistical significance for these false-positive readings were several orders of magnitude less than for the true-positive results in the patient group. To be clinically useful, other potential problems will need to be addressed. These include identifying acute infarcts in the presence of previous infarcts. Because this is an attenuation-based process, the algorithm currently makes no distinction between old and new infarcts. Also, areas of atrophy, calcification, and hemorrhage will affect the histogram distribution. More sophisticated algorithms could include morphologic feature analysis for sulcal effacement and relative loss of boundary information (ie, gray-white differentiation) to improve the specificity of the automated analysis methodologies. Improvements in image registration algorithms, including implementation of nonlinear warping algorithms and the use of a dedicated CT template, may increase the accuracy of the segmentation process. On-line implementation may assist physicians in the interpretation of hyperacute CT and should improve accuracy and interobserver reliability. We think that further diagnostic information can be garnered from CT scans obtained of patients with acute stroke that can help to identify areas of involvement and quantify vascular territory involvement. This information is critically needed for rapidly stratifying patients for the use of novel potentially life-saving therapies in cases of acute stroke.

Conclusion

We present an automated method for identifying potential areas of acute ischemia on CT scans. This approach can be extended to other brain regions and vascular territories and may aid in the interpretation of CT scans in cases of hyperacute stroke.

References

1. Torack R, Alcala H, Gado M, Burton R. **Correlative assay of computerized cranial tomography CCT, water content and specific gravity in normal and pathological postmortem brain.** *J Neurapathol Exp Neurol* 1976;35:385–392
2. Marks M. **CT in ischemic stroke.** *Neuroimaging Clin N Am* 1998; 8:515–523
3. von Kummer R, Meyding-Lamade U, Forsting M, et al. **Sensitivity and prognostic value of early CT in occlusion of the middle cerebral artery trunk.** *AJNR Am J Neuroradiol* 1994;15:9–18
4. Tomura N, Uemura K, Inugami A, Fujita H, Higano S, Shishido F. **Early CT finding in cerebral infarction: obscuration of the lentiform nucleus.** *Radiology* 1988;168:463–467
5. Truwit C, Barkowich A, Gean-Marton A, Hibri H, Norman D. **Loss of the insular ribbon: another early CT sign of acute middle cerebral artery infarction.** *Radiology* 1990;176:801–806
6. Tomsick T, Brott T, Olinger C, et al. **Hyperdense middle cerebral artery: incidence and quantitative significance.** *Neuroradiology* 1989;31:312–315
7. Wall S, Brant-Zawadski M, Jeffrey R, Barnes B. **High frequency CT findings within 24 hours after cerebral infarction.** *AJR Am J Roentgenol* 1982;138:307–311
8. von Kummer R, Allen K, Holle R, et al. **Acute stroke: usefulness of early CT findings before thrombolytic therapy.** *Radiology* 1997;205:327–333

9. Marks M, Holmgren E, Fox A, Patel S, Kummer RV, Froelich J. **Evaluation of early computed tomographic findings in acute ischemic stroke.** *Stroke* 1999;30:389–392
10. Hacke W, Kaste M, Fieschi C, et al. **Intravenous thrombolysis with recombinant tissue plasminogen activator for acute hemispheric stroke: The European Cooperative Acute Stroke Study (ECASS).** *JAMA* 1995;274:1017–1025
11. Hacke W, Kaste M, Fieschi C, et al. **Safety and efficacy of intravenous thrombolysis with recombinant tissue plasminogen activator in the treatment of acute hemispheric stroke.** *JAMA* 1995;274:1017–1025
12. Krieger DW, Demchuk AM, Kasner SE, Jauss M, Hantson L. **Early clinical and radiological predictors of fatal brain swelling in ischemic stroke.** *Stroke* 1999;30:287–292
13. Shinar D, Gross C, Hier D, et al. **Interobserver reliability in the interpretation of computed tomographic scans of stroke patients.** *Arch Neurol* 1987;44:149–155
14. Schriger D, Kalafut M, Starkman S, Krueger M, Saver J. **Cranial computed tomography interpretation in acute stroke: physician accuracy in determining eligibility for thrombolytic therapy.** *JAMA* 1998;279:1293–1297
15. Grotta J, Chiu D, Lu M, et al. **Agreement and variability in the interpretation of early CT changes in stroke patients qualifying for intravenous rtPA therapy.** *Stroke* 1999;30:1528–1533
16. von Kummer R, Holle R, Gizyska U, et al. **Interobserver agreement in assessing early CT signs of middle cerebral artery infarction.** *AJNR Am J Neuroradiol* 1996;17:1743–1748
17. Lev M, Farkas J, Gemmete J, et al. **Acute stroke: improved nonenhanced CT detection benefits of soft-copy interpretation by using variable window width and center level settings.** *Radiology* 1999;213:150–155
18. Bendszus M, Urbach H, Meyer B, Schulthieb R, Solymosi L. **Improved CT diagnosis of acute middle cerebral artery territory infarcts with density-difference analysis.** *Neuroradiology* 1997; 39:127–131
19. Talairach J, Tournoux P. ***Co-Planar Stereotaxic Atlas of the Human Brain: 3-Dimensional Proportional System: an Approach to Cerebral Imaging.*** New York: Thieme Medical Publishers; 1988
20. Friston K, Holmes A, Worsley K, Poline J, Frith C, Frackowiak R. **Statistical parametric maps in functional imaging: a general approach.** *Hum Brain Mapp* 1995;2:189–201
21. Friston K, Ashburner J, Poline J, Frith C, Heather J, Frackowiak R. **Spatial registration and normalization of images.** *Hum Brain Mapp* 1995;2:165–189
22. Kikinis R, Shenton M, Iosifescu D, et al. **A digital brain atlas for surgical planning, model driven segmentation and teaching.** *IEEE Trans Vis Comput Graph* 1996;2:2323–2241
23. Barber PA, Demchuk AM, Zhang J, Buchan AM. **Validity and reliability of a quantitative computed tomography score in predicting outcome of hyperacute stroke before thrombolytic therapy: ASPECTS Study Group: Alberta Stroke Programme Early CT Score.** *Lancet* 2000;355:1670–1674